Available online at www.sciencedirect.com
ScienceDirect
Journal of Sound and Vibration 323 (2009) 1–16
JOURNAL OF SOUND AND VIBRATION
www.elsevier.com/locate/jsvi

Active pendulum vibration absorbers with a spinning support

Shang-Teh Wu*

Department of Mechanical Engineering, National Yunlin University of Science and Technology, Touliu, Yunlin 640, Taiwan

Received 25 February 2008; received in revised form 30 October 2008; accepted 10 December 2008
Handling Editor: J. Lam
Available online 20 January 2009

Abstract

A novel pendulum vibration absorber with a rotational base is proposed for neutralization of vertical excitations. The characteristic frequency of the absorber can be dynamically tuned over a wide range by varying the rotational speed. The external disturbance is countered by the inertial force of the revolving mass, whose angular momentum is not affected by the external excitation. As a result minimal power is required to sustain the system in steady state. This paper first derives the characteristic frequency of the rotational pendulum as function of the rotational rate. A pair of symmetric pendulums are then installed on a primary structure subject to harmonic disturbances. It is shown how the pendulum absorber is capable of balancing the external excitation. Asymptotic stability of the linearized system is also proved. Numerical simulations are then conducted to illustrate the performance of the system. Finally a variant design resembling a fly-ball governor is presented; it has the merit of ensuring simultaneous motions of two symmetric rotational pendulums so that lateral oscillations are canceled. The proposed scheme is suitable for an active vibration control system where there is a constraint on the power or force capacity of a linear actuator.

1. Introduction

Pendulum vibration absorbers have been installed in high-rise buildings, bridges, and other civil structures to attenuate wind-excited vibrations [1,2]. Compared to a conventional vibration absorber made of a movable mass and a flexible member, a simple pendulum is more rugged, easily constructed, and suitable for heavy-duty jobs. The rolling-ball vibration absorber [3] can be considered to be a variant of the pendulum absorbers. However, such horizontally movable absorbers are rarely used in mechanical apparatuses for the following reasons. Firstly, the characteristic frequency of a simple pendulum is relatively low due to the length constraint. For example, in order to have a natural frequency larger than 3 Hz, the pendulum rod must be *shorter* than 3 cm. Secondly, since the characteristic frequency is fixed, a passive pendulum absorber is not suitable for excitations of time-varying frequencies. The third reason is that a simple gravitational pendulum can only counter horizontal vibrations. Other types of pendulum absorbers are available for attenuation of non-horizontal vibrations: the centrifugal pendulum absorber (see e.g. Refs. [4–6]) utilizes the rotational

*Tel.: +886 5 5342601x4111; fax: +886 5 5312062.
E-mail address: wust@yuntech.edu.tw

0022-460X/$ - see front matter © 2009 Elsevier Ltd. All rights reserved.
doi:10.1016/j.jsv.2008.12.017

Nomenclature

d	(harmonic) disturbance on the primary structure
d_0	amplitude of the disturbance
g	acceleration due to gravity
k_p	proportional gain for speed regulation
ℓ	length of the pendulum
m	lumped mass of the pendulum
m_0, k_0, b_0	mass, stiffness, and damping coefficient of the primary structure, respectively
m_1	summed mass of the balls in the fly-ball mechanism
m_2	mass of the slider in the fly-ball mechanism
p	deviation of angular speed ($\dot{\phi}$) from ω_0
q	deviation of θ from θ_0
u	torque exerted by the driving motor
x	displacement of the primary structure
θ, θ_0	angular displacement and equilibrium angle of the pendulum about a lateral axis, respectively
$\dot{\phi}$	rotational speed of the pendulum about the vertical axis
ω_0	target (constant) rotational speed of pendulum about the vertical axis
ω_n	characteristic frequency (rad/s) of the rotational pendulum

centrifugal field to generate a restoring force tangential to the rotor, thus capable of neutralizing torsional disturbances. In an *autoparametric* system [7–10], simple pendulums can be devised to absorb vertical vibrations from the primary structure if a stringent condition is satisfied. Such autoparametric resonance is due to nonlinear coupling between the primary structure and the pendulum subsystem. For quadratic nonlinearities, it requires that the natural frequencies of the primary structure, the pendulum absorber, and the external excitation be tuned in a specific ratio (2:1:2).

This paper proposes a rotational pendulum absorber for neutralization of vertical disturbances. The characteristic frequency of the pendulum absorber can be dynamically tuned over a wide range by adjusting the rotational speed. The proposed scheme has the benefits of low-power consumption of a passive vibration absorber and flexibility of an active device. While an electric motor is needed to turn the pendulum to a set speed, the external power required to sustain the system is minimal in steady state. This is because the external disturbance is not directly countered by the actuator but by the inertial force of the revolving mass, whose angular momentum is not affected by the external excitation. By contrast, in other active vibration control schemes (such as Refs. [11–14]), a portion of the external disturbance is directly balanced by the actuating force. The power capacity of the actuator must significantly increase with the magnitude of the disturbance.

The rest of the paper is arranged as follows. In Section 2 the characteristic frequency of a rotational pendulum is derived. The relationship between the frequency of vertical swings of the pendulum and its rotational speed is established. In Section 3 a symmetric pair of rotational pendulums are mounted on a single-free-degree-of-freedom primary structure which is subject to a harmonic disturbance. It is analyzed how the disturbance is neutralized by the rotational pendulums. Stability analysis is conducted on the linearized system where the rotational speed is regulated by a proportional control law. Section 4 presents the simulation results. Effects of the length, mass of the rotational pendulum and the magnitude, frequency of the external disturbance on the system performance are investigated. The feature that the rotational pendulum consumes minimal power in steady state is demonstrated and physically explained. Section 5 presents a variant design of the rotational pendulum, where a slider is used to guide the two symmetric pendulums, so that simultaneous motions are ensured. Section 6 is the concluding remarks.

2. Characteristic frequencies of a rotational pendulum

Fig. 1b depicts a pendulum revolving about a vertical axis, in contrast to a simple pendulum swinging horizontally (Fig. 1a). For simplicity the rotational pendulum is assumed to have a length ℓ and a lumped mass m at the tip. The damping and frictional forces are neglected. In this section we will investigate the natural frequency of the rotational pendulum when its base is turning at a constant speed, denoted by ω_0.

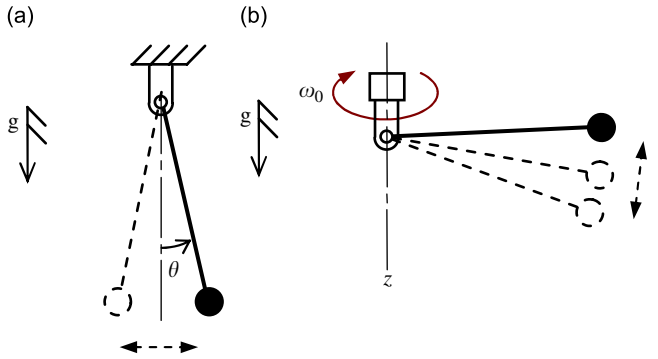

Fig. 1. (a) Horizontally swinging pendulum; (b) vertically swinging pendulum with a revolving support.

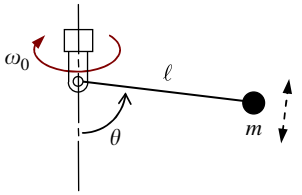

Fig. 2. Rotational pendulum at a constant speed.

The governing equation of the rotational pendulum can be derived using the Lagrange equation. Referring to Fig. 2, the kinetic energy and potential energy are, respectively,

$$T = \tfrac{1}{2}m[(\ell\dot{\theta})^2 + (\ell\omega_0 \sin\theta)^2] \tag{1}$$

$$V = mg\ell(1 - \cos\theta) \tag{2}$$

where θ is the angular displacement of the pendulum in the vertical direction. Let

$$\mathscr{L} = T - V \tag{3}$$

From the Lagrange equation,

$$\frac{\mathrm{d}}{\mathrm{d}t}\left(\frac{\partial\mathscr{L}}{\partial\dot{\theta}}\right) - \frac{\partial\mathscr{L}}{\partial\theta} = 0 \tag{4}$$

we have

$$m\ell^2\ddot{\theta} + mg\ell \sin\theta - \tfrac{1}{2}m\ell^2\omega_0^2 \sin 2\theta = 0 \tag{5}$$

Let $\ddot{\theta} = 0$ in Eq. (5). The equilibrium angle for the pendulum, denoted by θ_0, satisfies

$$mg\ell \sin\theta_0 - \tfrac{1}{2}m\ell^2\omega_0^2 \sin 2\theta_0 = 0 \tag{6}$$

Since $\sin 2\theta_0 = 2\sin\theta_0\cos\theta_0$, Eq. (6) can be reduced to

$$\theta_0 = 0 \quad \text{if } \omega_0 = 0 \tag{7}$$

$$g - \ell\omega_0^2\cos\theta_0 = 0 \quad \text{if } \omega_0 \neq 0 \tag{8}$$

Denote q to be a small deviation of θ from the equilibrium, i.e.,

$$q = \theta - \theta_0 \tag{9}$$

From Eqs. (5) and (6) the linearized dynamic equation about the equilibrium can be calculated to be

$$m\ell^2\ddot{q} + (mg\ell\cos\theta_0 - m\ell^2\omega_0^2\cos 2\theta_0)q = 0 \tag{10}$$

If $\omega_0 = 0$ (so that $\theta_0 = 0$), Eq. (10) reduces to

$$\ell\ddot{q} + gq = 0, \tag{11}$$

which is the linearized equation of a simple pendulum.

Now consider the non-trivial case where $\omega_0 \neq 0$. Substitution of Eq. (8) into Eq. (10) leads to

$$\ddot{q} + (\cos^2\theta_0 - \cos 2\theta_0)\omega_0^2 q = 0 \tag{12}$$

Using the identity that $\cos 2\theta_0 = \cos^2\theta_0 - \sin^2\theta_0$, Eq. (12) can be expressed as

$$\ddot{q} + \omega_0^2 \sin^2\theta_0\, q = 0 \tag{13}$$

The characteristic frequency (ω_n) of the rotational pendulum is thus shown to be

$$\omega_n = \omega_0 \sin\theta_0 \tag{14}$$

Furthermore, a solution of ω_0 can be found in terms of ω_n: from Eq. (8),

$$\left(\frac{g}{\ell\omega_0}\right)^2 = \omega_0^2 \cos^2\theta_0 \tag{15}$$

Squaring both sides of Eq. (14) and adding the result to Eq. (15) yield

$$\omega_n^2 + \left(\frac{g}{\ell\omega_0}\right)^2 = \omega_0^2 \tag{16}$$

It can be expressed as a quadratic equation in ω_0^2:

$$\ell^2(\omega_0^2)^2 - \ell^2\omega_n^2\omega_0^2 - g^2 = 0 \tag{17}$$

Solving Eq. (17) for ω_0^2 yields

$$\omega_0^2 = \frac{\omega_n^2 + \sqrt{\omega_n^4 + 4(g/\ell)^2}}{2} \tag{18}$$

Fig. 3 shows the equilibrium angle and the normalized natural frequency of the rotational pendulum as a function of the normalized angular speed. It is seen that for the rotational pendulum to have a non-zero equilibrium, the angular speed must be larger than the natural frequency of a simple pendulum ($\sqrt{g/\ell}$). Moreover, the natural frequency almost matches the angular speed when the later is larger than two times the frequency of a corresponding simple pendulum.

3. Rotational pendulum as a vibration absorber

A single-degree-of-freedom primary structure equipped with a symmetric pair of rotational pendulums will be analyzed in this section. As shown in Fig. 4, the structure is subject to a harmonic disturbance possibly caused by a rotary machine. The pendulums are supported by a shaft which is driven by a motor. The mass, stiffness, and damping coefficient of the primary structure are, respectively, m_0, k_0, and b_0, as indicated in Fig. 5. Each of the two symmetric pendulums has a length of ℓ and a lumped mass of $\frac{1}{2}m$. Governing equations of the system are derived as follows.

The kinetic and potential energy of the system are, respectively, obtained to be

$$T = \tfrac{1}{2}m[(\ell\dot{\theta}\sin\theta + \dot{x})^2 + (\ell\dot{\theta}\cos\theta)^2 + (\ell\dot{\phi}\sin\theta)^2] + \tfrac{1}{2}m_0\dot{x}^2 \tag{19}$$

$$V = mg\ell(1 - \cos\theta) + \tfrac{1}{2}k_0x^2 \tag{20}$$

where $\dot{\phi}$ is the rotational speed of the pendulums. Note that the term $(m_0 + m)gx$ is not included in V, since the origin of x is taken to be the equilibrium position.

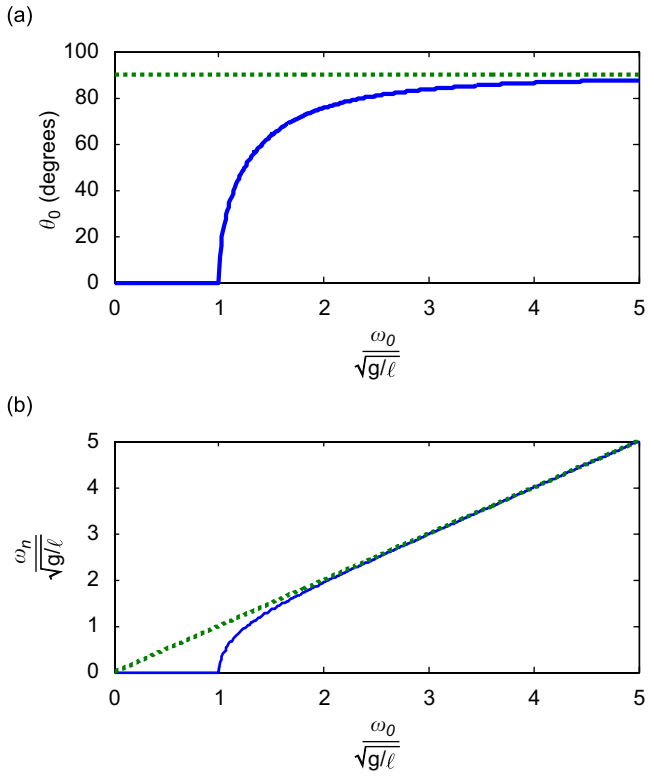

Fig. 3. (a) Equilibrium angle versus rotational speed for the pendulum absorber; (b) natural frequency versus rotational speed.

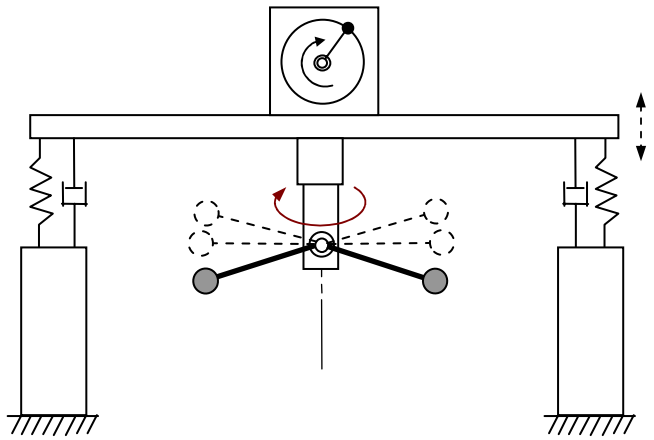

Fig. 4. Rotational pendulums installed on a primary structure subject to a harmonic disturbance.

3.1. Constant rotational speeds

First we consider the situation in which the rotational speed is kept constant, i.e., $\dot{\phi} = \omega_0$. Two degrees of freedom remain in this system, namely the oscillation of the primary structure and the up-down swing of the pendulum.

Define $\mathscr{L}$ as in Eq. (3), where T and V are given in Eqs. (19) and (20). The Lagrange equations for the x and θ coordinates are derived below.

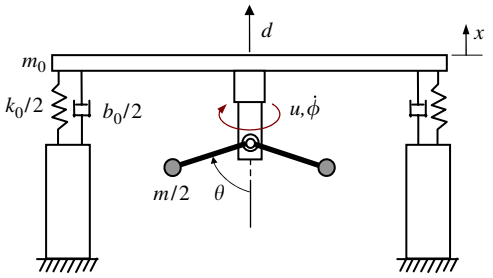

Fig. 5. Coordinate notations and parameters of the vibration control system.

Using Eq. (4) we have

$$m\ell^2\ddot{\theta} + m\ell(\ddot{x} + g)\sin\theta - \tfrac{1}{2}m\ell^2\dot{\phi}^2\sin 2\theta = 0 \tag{21}$$

And from

$$\frac{\mathrm{d}}{\mathrm{d}t}\left(\frac{\partial \mathscr{L}}{\partial \dot{x}}\right) - \frac{\partial \mathscr{L}}{\partial x} = -b_0\dot{x} + d \tag{22}$$

where d is the harmonic disturbance, we have

$$m\ell\ddot{\theta}\sin\theta + (m + m_0)\ddot{x} + m\ell\dot{\theta}^2\cos\theta + k_0 x + b_0\dot{x} = d \tag{23}$$

Similar to Eq. (13), Eq. (21) is linearized about the equilibrium angle (θ_0) to be

$$m\ell^2\,\ddot{q} + (m\ell\sin\theta_0)\ddot{x} + (m\ell^2\omega_0^2\sin^2\theta_0)q = 0 \tag{24}$$

Note that $\dot{\phi}$ is replaced by ω_0 since it is assumed to be a constant. Eq. (23) can also be readily linearized to be

$$(m\ell\sin\theta_0)\ddot{q} + (m + m_0)\ddot{x} + k_0 x + b_0\dot{x} = d \tag{25}$$

Eqs. (24) and (25) can be written in matrix form to be

$$\mathbf{M}\ddot{\mathbf{z}} + \mathbf{K}\mathbf{z} + \mathbf{C}\dot{\mathbf{z}} = [0 \;\; d]^{\mathrm{T}} \tag{26}$$

where $\mathbf{z} = [q \;\; x]^{\mathrm{T}}$,

$$\mathbf{M} = \begin{bmatrix} m\ell^2 & m\ell\sin\theta_0 \\ m\ell\sin\theta_0 & m + m_0 \end{bmatrix}, \quad \mathbf{K} = \begin{bmatrix} m\ell^2\omega_0^2\sin^2\theta_0 & 0 \\ 0 & k_0 \end{bmatrix} \tag{27}$$

and

$$\mathbf{C} = \begin{bmatrix} 0 & 0 \\ 0 & b_0 \end{bmatrix} \tag{28}$$

Since $\mathbf{M}$ and $\mathbf{K}$ are symmetric and positive definite matrices, and $\mathbf{C}$ is a positive semi-definite matrix, Eq. (26) depicts a two-degree-of-freedom passive structure under forced vibration. Let

$$d = d_0\sin(\omega_n t + \psi) \tag{29}$$

where d_0 is the amplitude and ψ is an arbitrary phase angle. If ω_0 is chosen according to Eq. (18), we have $\omega_n = \omega_0\sin\theta_0$. The steady-state solution to Eq. (26) will be $x = \dot{x} = 0$, and

$$q = \alpha\sin(\omega_n t + \psi) \tag{30}$$

where

$$\alpha = -\frac{d_0}{m\ell\omega_n^2\sin\theta_0} \tag{31}$$

The solution can be checked by substitution of Eqs. (30) and (31), and $x = \dot{x} = 0$ back into Eqs. (24) and (25). It is thus shown that the rotational pendulum acts as a vibration absorber to a harmonic disturbance whose frequency is equal to $\omega_0 \sin\theta_0$.

3.2. Proportional control

In practice the rotational speed is not a constant but can be regulated at the desired speed by a simple proportional control law, that is

$$u = k_p(\omega_0 - \dot{\phi}) \tag{32}$$

where u is the torque exerted on the shaft supporting the pendulums, and k_p is a positive constant. The system now has one more degree of freedom. It will be shown below that the linearized system of the three-degree-of-freedom system is asymptotically stable.

From

$$\frac{\mathrm{d}}{\mathrm{d}t}\left(\frac{\partial \mathscr{L}}{\partial \dot{\phi}}\right) - \frac{\partial \mathscr{L}}{\partial \phi} = u, \tag{33}$$

we have

$$m\ell^2(\ddot{\phi}\sin^2\theta + \dot{\phi}\dot{\theta}\sin 2\theta) = u \tag{34}$$

Denote the deviation of the angular speed from ω_0 to be p, i.e.,

$$p = \dot{\phi} - \omega_0 \tag{35}$$

From the definitions of p and q, we have

$$\ddot{\phi} = \dot{p} \tag{36}$$

$$\dot{\theta} = \dot{q} \tag{37}$$

$$u = -k_p p \tag{38}$$

Substituting Eqs. (35)–(38) into Eq. (34) and dropping the nonlinear terms lead to

$$(m\ell^2\sin^2\theta_0)\dot{p} + (m\ell^2\omega_0\sin 2\theta_0)\dot{q} = -k_p p \tag{39}$$

As shown in the Appendix, the linearized equation of Eq. (21) can be derived to be

$$m\ell^2\,\ddot{q} + (m\ell\sin\theta_0)\ddot{x} - (m\ell^2\omega_0\sin 2\theta_0)p + (m\ell^2\omega_0^2\sin^2\theta_0)q = 0 \tag{40}$$

The linearized equation for Eq. (23) is

$$(m\ell\sin\theta_0)\ddot{q} + (m+m_0)\ddot{x} + k_0 x + b_0\dot{x} = 0 \tag{41}$$

which is the same as Eq. (25) except that the forcing term d is dropped.

Similar to Eq. (26), Eqs. (40) and (41) can be expressed in matrix form to be

$$\mathbf{M}\ddot{\mathbf{z}} + \mathbf{K}\mathbf{z} + \mathbf{C}\dot{\mathbf{z}} - \mathbf{D}p = \mathbf{0} \tag{42}$$

where $\mathbf{M}$, $\mathbf{K}$, and $\mathbf{C}$ are as defined previously, and

$$\mathbf{D} = \begin{bmatrix} m\ell^2\omega_0\sin 2\theta_0 \\ 0 \end{bmatrix} \tag{43}$$

3.3. Stability analysis of the linearized system

With an appropriate Lyapunov function it will be proved that the linearized system governed by Eqs. (39) and (42) is asymptotically stable.

Let

$$V_L = \tfrac{1}{2}\dot{\mathbf{z}}^{\mathrm{T}}\mathbf{M}\dot{\mathbf{z}} + \tfrac{1}{2}\mathbf{z}^{\mathrm{T}}\mathbf{K}\mathbf{z} + \tfrac{1}{2}\gamma p^2 \tag{44}$$

where $\gamma = m\ell^2 \sin^2\theta_0$. Since $\mathbf{M}$ and $\mathbf{K}$ are positive definite, and $\gamma > 0$, it follows that $V_L \geqslant 0$; in other words, V_L is *lower bounded*. The time derivative of V_L is calculated to be

$$\dot{V}_L = -\dot{\mathbf{z}}^{\mathrm{T}}\mathbf{M}\ddot{\mathbf{z}} + \mathbf{z}^{\mathrm{T}}\mathbf{K}\dot{\mathbf{z}} + \gamma p\dot{p} \tag{45}$$

$$= \dot{\mathbf{z}}^{\mathrm{T}}(-\mathbf{K}\mathbf{z} - \mathbf{C}\dot{\mathbf{z}} + \mathbf{D}p) + \mathbf{z}^{\mathrm{T}}\mathbf{K}\dot{\mathbf{z}} + \gamma p\left(-\frac{m\ell^2\omega_0 \sin 2\theta_0}{\gamma}\,\dot{q} - \frac{k_p}{\gamma}\,p\right) \tag{46}$$

$$= -\dot{\mathbf{z}}^{\mathrm{T}}\mathbf{C}\dot{\mathbf{z}} - k_p p^2 \tag{47}$$

$$= -b_0\dot{x}^2 - k_p p^2 \tag{48}$$

Eq. (46) is obtained using Eqs. (42) and (39) to substitute for $\ddot{\mathbf{z}}$ and $\dot{p}$, respectively, in Eq. (45). Note that in Eq. (46), the term $\dot{\mathbf{z}}^{\mathrm{T}}\mathbf{D}p$ cancels with the term associated with $\dot{q}$.

Since V_L is lower bounded and its time derivative, $\dot{V}_L$, is less than or equal to zero, it follows that $\dot{V}_L$ must tend to zero, expressed as $\dot{V}_L \to 0$. From Eq. (48) we have $\dot{x} \to 0$ and $p \to 0$, which also imply $\ddot{x} \to 0$ and $\dot{p} \to 0$. Substitution of $\dot{x} = \ddot{x} = \dot{p} = p = 0$ back into Eqs. (39) and (42) leads to $\mathbf{z} = \dot{\mathbf{z}} = \mathbf{0}$. It is thus proved that the linearized system is asymptotically stable.

Note that while the primary structure is assumed to have only one degree of freedom, the stability analysis can be readily generalized to structures with multiple degrees of freedom. The difference would be in the mass and stiffness matrices ($\mathbf{M}$ and $\mathbf{K}$), which are symmetric and positive definite for a passive mechanical structure.

4. Simulation results

Numerical simulations are conducted to test the performance of the rotational pendulum absorber. The simulated system, as depicted in Fig. 5, is governed by the original nonlinear dynamic equations, namely Eqs. (21), (23), and (34). The rotational speed is regulated by the proportional law of Eq. (32). The parameters of the system are assumed to be: $m_0 = 10\,\mathrm{kg}$, $k_0 = 1000\,\mathrm{N/m}$, $b_0 = 40\,\mathrm{N\,s/m}$; the lumped mass of the pendulum (m) is 2 kg, and the length (ℓ) is 0.2 m. The frequency of the disturbance is 10 Hz (62.8 rad/s). The rotational speed of the pendulum will be regulated at the value calculated by Eq. (18). Two different disturbance amplitudes are simulated.

4.1. Case A: $d_0 = 50\,N$

Figs. 6 and 7 show the results for $d_0 = 50\,\mathrm{N}$. (Without vibration control, the primary structure would oscillate at an amplitude of about 0.001 m.) In the simulation the proportional gain k_p is equal to 0.1 for $t = 0$–15 s, and is zero after 15 s. (That is, the control power is turned off after 15 s.) It is seen in Fig. 6 that vibrations of the primary structure are nearly eliminated by the rotational pendulum. Fig. 7 shows that in steady state the vertical swing of the pendulum is 180° out of phase with the disturbance so that the two forces cancel each other. Note that the pendulum absorber continues to function well even after the control input is turned off. This will be further elaborated later.

4.2. Case B: $d_0 = 500\,N$

In the second simulation the amplitude of the disturbance is raised to 500 N. (For this amplitude the primary structure would oscillate at an amplitude of about 0.01 m without vibration control.) The proportional gain is set in the same way as in the previous case. Figs. 8 and 9 show the simulation results. It is seen that oscillations of the primary structure are also neutralized near perfectly. As expected the pendulum undergoes larger swing, since the magnitude of the disturbance is 10 times as large as the previous case.

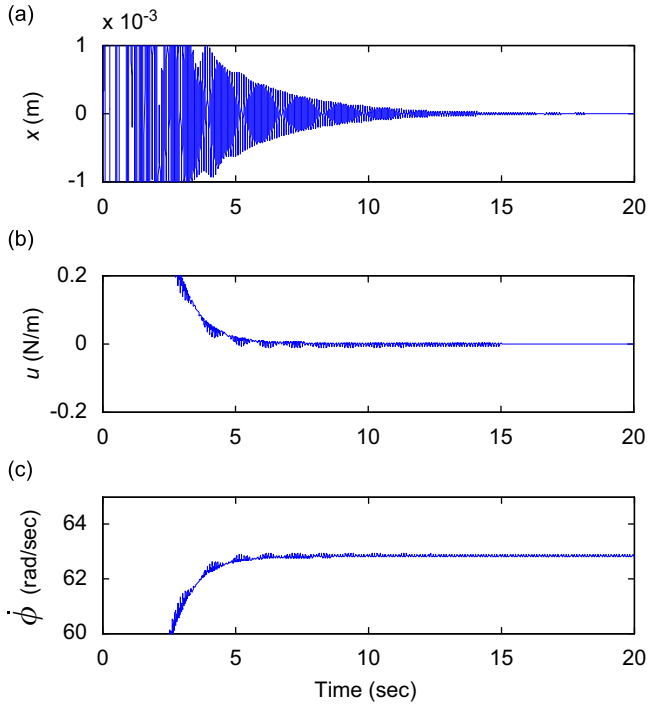

Fig. 6. Time response of the system for $d_0 = 50$ N: (a) vibrations of the primary structure; (b) torque applied to the shaft; (c) rotational speed.

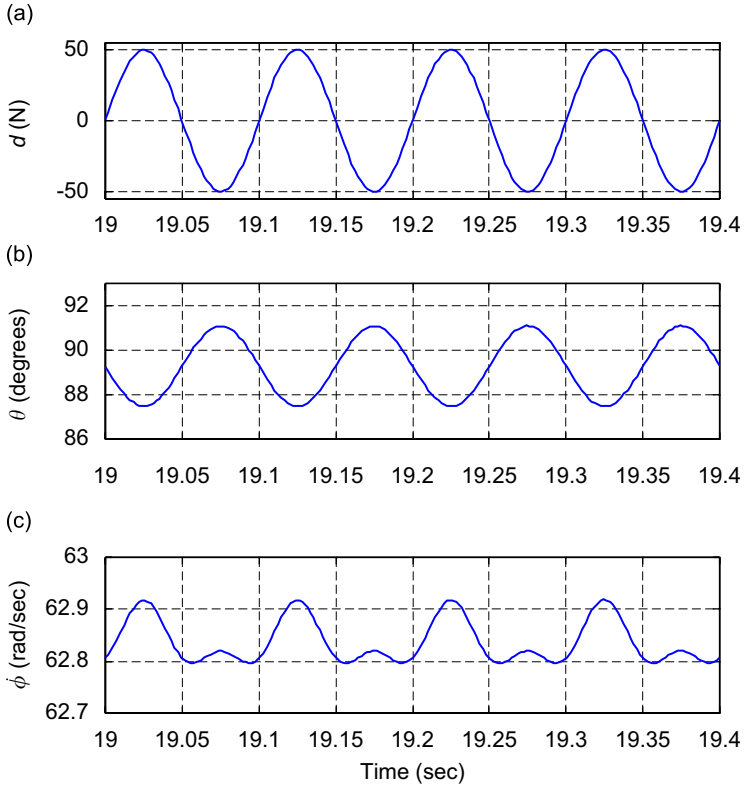

Fig. 7. Close-ups of steady-state response: (a) external disturbance; (b) up–down swing of the pendulum; (c) rotational speed.

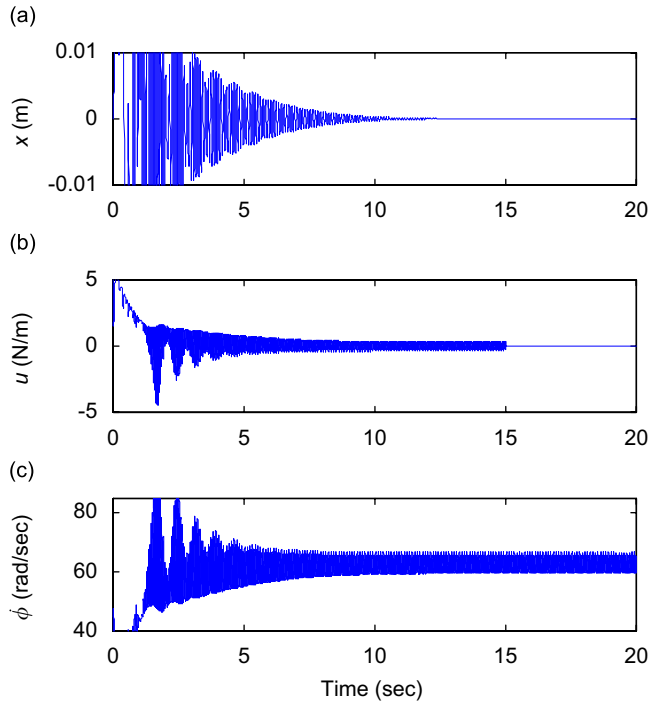

Fig. 8. Time response of the system for $d_0 = 500$ N: (a) vibrations of the primary structure; (b) torque applied to the shaft; (c) rotational speed.

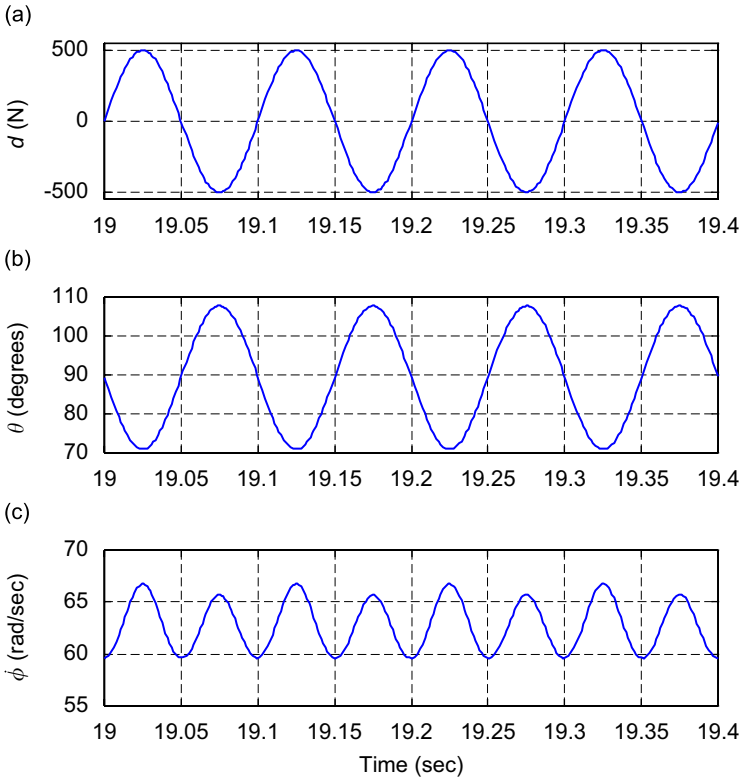

Fig. 9. Close-ups of steady-state response: (a) external disturbance; (b) up–down swing of the pendulum; (c) rotational speed.

4.3. Frequency response

The frequency response of the linearized system (Eqs. (25), (39) and (40)) with d as input and x as output is plotted in Fig. 10. The angular speed (ω_0) is selected for a characteristic frequency of 10 Hz; that is, $\omega_n = 20\pi\,(\mathrm{rad/s})$ in Eq. (18). The parameters are the same as used in the above time-domain simulations. The dashed curve in Fig. 10 is the response for the uncontrolled system, in which the rotational pendulum is removed and the pendulum weight is added to the primary body (for a fair comparison). It is seen that the solid curve has a dip at 10 Hz, indicating complete neutralization of disturbance at this frequency.

4.4. Parametric analysis

The effect of the mass, length, and rotational speed of the pendulum is investigated by numerically experimenting on the system, varying one parameter at a time. Effectiveness of the rotational pendulum can be measured by the *attenuation ratio*, defined as the ratio of the magnitude of the residual vibrations of the primary structure when the absorber is inactive (i.e., when the pendulum is vertically down and non-rotating) *to* the magnitude when the absorber is active. For example, in Case A the magnitude of x without vibration control is 0.001 m, while it tends to be 3.7×10^{-6} m with vibration control. The attenuation ratio would be $0.001/3.7 \times 10^{-6} = 270$. Figs. 11 and 12 show the attenuation ratio as a function of the magnitude of the disturbance. It is seen that the smaller the disturbance magnitude, the higher the attenuation ratio. This is because with large d_0 the pendulum must undergo large swinging to counteract the disturbance, resulting in significant deviation from the linearized dynamics. On the other hand, increasing the length of the pendulum substantially improves the attenuation ratio, because with longer arms the angular up–down swinging is smaller for the same disturbance magnitude. Comparing Figs. 11 and 12, one can see that the absorber is more effective for higher disturbance frequency. This is because with larger rotational speed the pendulum undergoes smaller up–down swinging for the same magnitude of disturbance. Moreover, from Fig. 3 the equilibrium angle of the pendulum is closer to 90°, the ideal horizontal posture, for higher rotational speed.

To examine the effect of the pendulum mass, the attenuation ratio is measured by varying m from 0.5 to 3 kg for $d_0 = 500$ N and for a disturbance frequency of 10 Hz. The result is shown in Fig. 13, where it is seen that the pendulum mass also has a significant effect on the attenuation ratio: the larger the mass, the higher the attenuation ratio.

To summarize, the rotational pendulum is most effective for high-frequency disturbances. For low-frequency or high-magnitude disturbances, either the length or the mass of the pendulum must be increased. It is interesting to note that, given $d_0 = 500$ N and $m = 2$ kg, the length of the pendulum required to achieve an

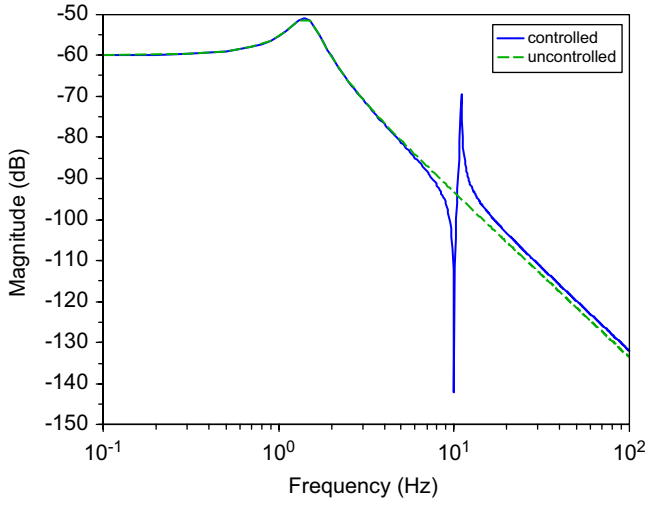

Fig. 10. Frequency response of the system with d as input and x as output. The dashed curve is for the uncontrolled system.

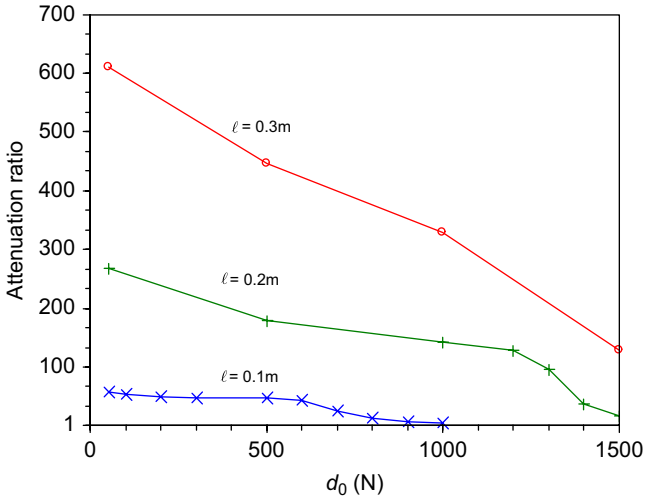

Fig. 11. Attenuation ratio versus disturbance magnitude for an excitation frequency of 10 Hz.

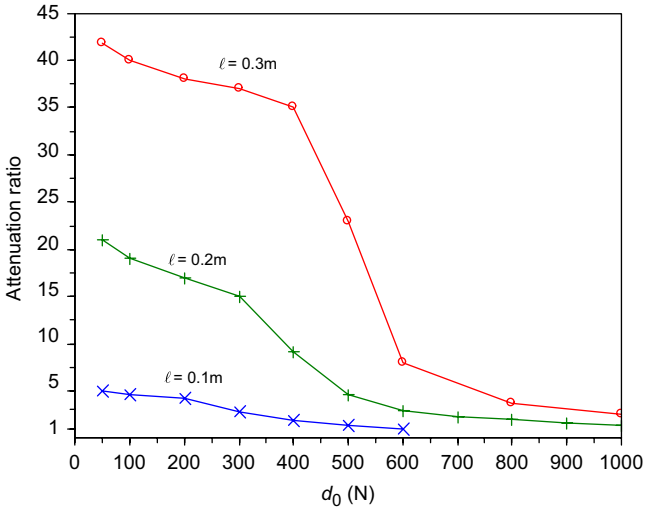

Fig. 12. Attenuation ratio versus disturbance magnitude for an excitation frequency of 5 Hz.

attenuation ratio of 100 is 0.46 m for an excitation frequency of 5 Hz; it is reduced to 0.15 m for a frequency of 10 Hz. For frequencies of 20 and 30 Hz, the length is further reduced to 0.05 and 0.031 m, respectively.

4.5. *Applied torque and power input*

In the simulations the torque applied to the rotational shaft is set to zero after 15 s, but the pendulum maintains its rotation and keeps functioning well. In other words, once the pendulum reaches the set speed, it becomes self-functional without power input. This feature is explained below.

If air resistance and frictional force on the rotary parts are neglected, as are assumed in the simulations, the angular momentum of the system in the vertical direction is *invariant* after the torque is set to zero. This is because none of the gravitational force, the linear damping and spring force, or the harmonic disturbance has a *moment* component in the vertical direction. As a result, when the arm of the pendulum *extends* horizontally (as θ is closer to 90 °), its angular speed *decreases;* when the arm *contracts* (as θ deviates away from 90 °),

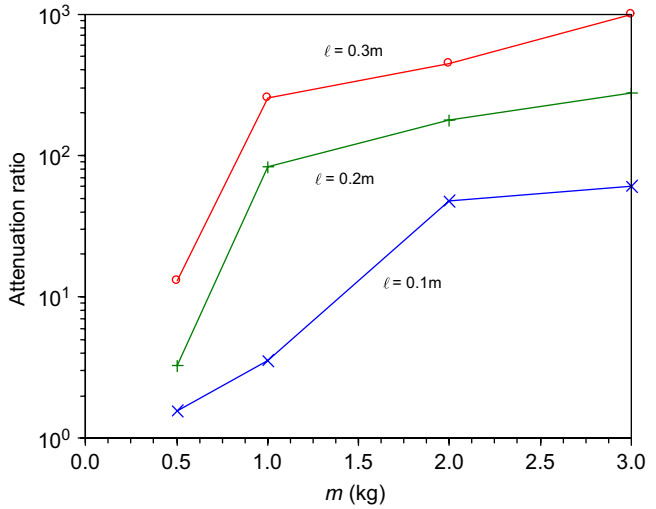

Fig. 13. Attenuation ratio versus pendulum mass for an excitation frequency of 10 Hz and disturbance magnitude of 500 N.

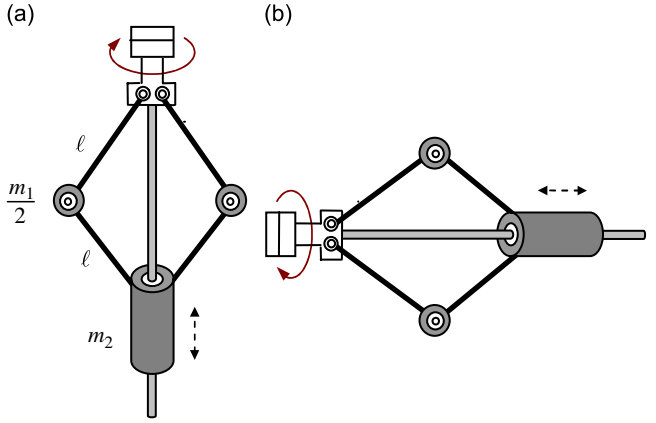

Fig. 14. A "fly-ball-governor" design that ensures symmetric motions of the two pendulums: (a) for vertical vibrations; (b) for horizontal vibrations.

its angular speed *increases* in such a way that the angular momentum remains constant. This phenomenon is illustrated in Figs. 7b, c and 9b, c.

In practice minimal power is required to compensate for air drag and frictions. However, the sustaining power is largely *independent* of the external excitation. This is in contrast to most active vibration control techniques in which a linear actuator counters the disturbing force directly, so that the capacity of the actuator must be proportional to the magnitude of disturbances.

5. Design issue

Fig. 14 shows a variant design of the rotational pendulum. It resembles a fly-ball governor. The two symmetric pendulums are constrained to move simultaneously by the slider. If the inertia of the slider is much smaller than the sum of the pendulums, i.e., $m_2 \ll m_1$, this *fly-ball* mechanism is equivalent to the rotational pendulum. However, it has the benefit of ensuring symmetric motion for the two pendulums so that lateral oscillations are canceled. The mechanism can also be tilted to tackle non-vertical disturbances, as shown in Fig. 14b.

The characteristic equation for the fly-ball mechanism can be developed in the same way as for the original rotational pendulum. For completeness it is presented below.

At constant rotation, the kinetic energy and the potential energy are, respectively,

$$T = \tfrac{1}{2}m_1[(\ell\dot{\theta})^2 + (\ell\omega_0 \sin\theta)^2] + \tfrac{1}{2}m_2(2\ell\dot{\theta}\sin\theta)^2 \tag{49}$$

$$V = m_1 g\ell(1 - \cos\theta) + 2m_2 g\ell(1 - \cos\theta) \tag{50}$$

where the rotational inertia of the slider has been neglected.

Similar to Eq. (5), the governing equation can be derived to be

$$(m_1 + 4m_2 \sin^2\theta)\ell^2\ddot{\theta} + (m_1 + 2m_2)g\ell \sin\theta + 4m_2\ell^2\dot{\theta}^2 \sin 2\theta - \tfrac{1}{2}m_1\ell^2\omega_0^2 \sin 2\theta = 0 \tag{51}$$

Compared to Eq. (8), at equilibrium

$$(m_1 + 2m_2)g - m_1\ell\omega_0^2 \cos\theta_0 = 0 \quad \text{if } \omega_0 \neq 0 \tag{52}$$

And similar to Eq. (13), the characteristic equation can be derived to be

$$(m_1 + 4m_2 \sin^2\theta_0)\ddot{q} + m_1\omega_0^2 \sin^2\theta_0 q = 0 \tag{53}$$

The characteristic frequency of the fly-ball mechanism is thus obtained to be

$$\omega_n = \omega_0 \sin\theta_0 \sqrt{\frac{m_1}{m_1 + 4m_2 \sin^2\theta_0}} \tag{54}$$

A closed-form formula relating ω_0 to ω_n similar to Eq. (18) may not be available. However, the relations can be obtained by numerically solving Eqs. (52) and (54), as shown in Fig. 15. In this figure, the normalized rotational speeds are plotted against the normalized characteristic frequency for m_2/m_1 varying from 0 to 5. Note that the curve for $m_2/m_1 = 0$ is governed by Eq. (18).

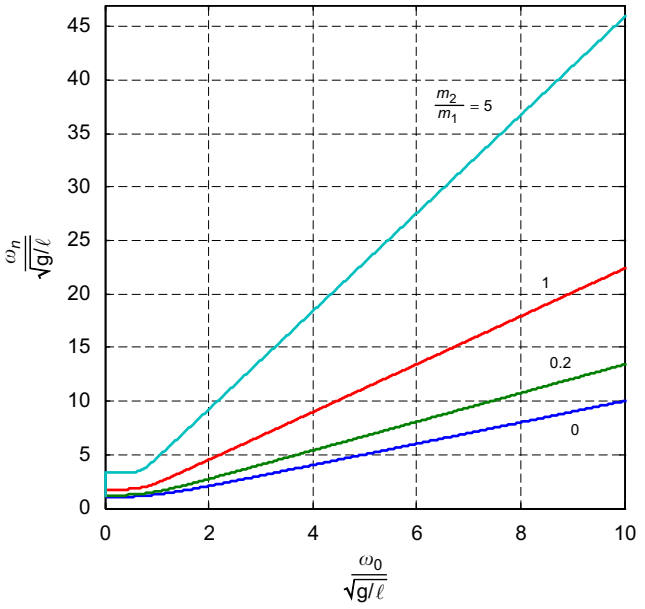

Fig. 15. Rotational speed versus characteristic frequency of the fly-ball mechanism for $m_2/m_1 = 0{\sim}5$. The bottom curve is governed by Eq. (18).

6. Conclusions

A pendulum with a spinning base is shown to be capable of neutralizing a vertical, harmonic excitation. The characteristic frequency of the rotational pendulum can be dynamically tuned over a wide range. Compared to a centrifugal pendulum absorber, in which the forward motion (i.e., the tangential velocity) of the pendulum is parallel to, and therefore strongly coupled with, its back-and-forth swings, the up–down oscillation of the rotational pendulum is better decoupled with its forward movement since the two motions are perpendicular to each other. The proposed scheme utilizes the inertial force of a moving object to balance the external disturbance, which has no effect on the angular momentum of the pendulum. As a result, except for the need to compensate for air drag and rotational frictions, no external power is required to sustain the system. The scheme is therefore suitable for an active vibration control system where energy consumption is a concern and there is a constraint on the power or force capacity of a linear actuator.

Appendix A. Derivation of Eq. (40)

For Eq. (21), the third term on the left-hand side is expanded to be

$$\begin{aligned} -\tfrac{1}{2}m\ell^2\dot{\phi}^2\sin 2\theta &= -\tfrac{1}{2}m\ell^2(\omega_0+p)^2\sin 2(\theta_0+q)\\ &\doteq -\tfrac{1}{2}m\ell^2(\omega_0^2\sin 2\theta_0 + 2p\omega_0\sin 2\theta_0 + 2q\omega_0^2\cos 2\theta_0)\\ &= -\tfrac{1}{2}m\ell^2(\omega_0^2\sin 2\theta_0 + 2p\omega_0\sin 2\theta_0 + 2q\omega_0^2(\cos^2\theta_0 - \sin^2\theta_0)) \end{aligned} \tag{55}$$

And the term associated with g in Eq. (21) is expanded to be

$$\begin{aligned} m\ell g\sin\theta &= m\ell g\sin(\theta_0+q)\\ &\doteq m\ell g(\sin\theta_0 + q\cos\theta_0) \end{aligned} \tag{56}$$

From Eq. (8),

$$g = \ell\omega_0^2\cos\theta_0 \tag{57}$$

Substitution of Eq. (57) into Eq. (56) yields

$$m\ell g\sin\theta \doteq \tfrac{1}{2}m\ell^2(\omega_0^2\sin 2\theta_0 + 2q\omega_0^2\cos^2\theta_0) \tag{58}$$

which cancel with the corresponding terms in Eq. (55). Thus Eq. (40) results.

References

[1] T. Nagase, T. Hisatoku, Tuned-pendulum mass damper installed in crystal tower, *The Structural Design of Tall Buildings* 1 (1992) 35–56.

[2] O. Fischer, Wind-excited vibrations: solution by passive dynamic vibration absorbers of different types, *Journal of Wind Engineering & Industrial Aerodynamics* 95 (2007) 1028–1039.

[3] M. Pirner, Actual behaviour of a ball vibration absorber, *Journal of Wind Engineering and Industrial Aerodynamics* 90 (2002) 987–1005.

[4] W. Thomson, *Theory of Vibration with Applications*, fifth ed., Prentice Hall, New Jersey, 1998, pp. 145–147.

[5] A.S. Alsuwaiyan, S.W. Shaw, Performance and dynamic stability of general-path centrifugal pendulum vibration absorbers, *Journal of Sound and Vibration* 252 (5) (2002) 791–815.

[6] B. Demeulenaere, P. Spaepen, J. De Schutter, Input torque balancing using a cam-based centrifugal pendulum: design procedure and example, *Journal of Sound and Vibration* 283 (1–2) (2005) 1–20.

[7] O. Cuvalci, A. Ertas, Pendulum as vibration absorber for flexible structures: experiments and theory, *Journal of vibration and acoustics* 118 (4) (1996) 558–566.

[8] A. Tondl, T. Ruijgrok, F. Verhulst, R. Nabergoj, *Autoparametric Resonance in Mechanical Systems*, Cambridge University Press, Cambridge, UK, 2000.

[9] A. Vyas, A.K. Bajaj, Dynamics of autoparametric vibration absorbers using multiple pendulums, *Journal of Sound and Vibration* 246 (1) (2001) 115–135.

[10] M. Yaman, S. Sen, Determining the effect of detuning parameters on the absorption region for a coupled nonlinear system of varying orientation, *Journal of Sound and Vibration* 300 (2007) 330–344.

[11] M. Yasuda, R. Gu, O. Nishihara, H. Matsuhisa, K. Ukai, M. Kondo, Development of anti-resonance enforced active vibration absorber system, *JSME International Journal, Series C* 39 (3) (1996) 464–469.
[12] H. Elmali, M. Renzulli, N. Olgac, Experimental comparison of delayed resonator and PD controlled vibration absorbers using electromagnetic actuators, *ASME Journal of Dynamic Systems, Measurement, and Control* 122 (2000) 514–520.
[13] Y.-D. Chen, C.-C. Fuh, P.-C. Tung, Application of voice coil motors in active dynamic vibration absorbers, *IEEE Transactions on Magnetics* 41 (3) (2005) 1149–1154.
[14] S.-T. Wu, Y.-Y. Chiu, Y.-C. Yeh, Hybrid vibration absorber with virtual passive devices, *Journal of Sound and Vibration* 299 (1–2) (2007) 247–260.